JOURNAL OF GUIDANCE, CONTROL, AND DYNAMICS
Vol. 29, No. 5, September–October 2006

Optimization and Implementation of Periodic Cruise for a Hypersonic Vehicle

Robert H. Chen,* Walton R. Williamson,† and Jason L. Speyer‡
SySense Inc., Burbank, California 91502
and
Hussein Youssef§ and Rajiv Chowdhry‖
Lockheed Martin Aeronautics Company, Palmdale, California 93599

DOI: 10.2514/1.19361

The optimal cruise trajectory for a detail designed hypersonic waverider vehicle is determined. Two possible local extrema are found representing the steady-state and periodic cruise trajectories. The optimal steady-state cruise is determined by minimizing the instantaneous fuel rate per distance subject to the dynamics being in equilibrium. The approximately optimal periodic cruise is determined by minimizing the fuel used over an optimal range period subject to a periodicity condition on the initial and terminal values of the altitude, velocity, and flight path angle, assuming that the vehicle weight is given and held fixed over the range period. It is shown that if a door is placed over the inlet during the power-off phase, increasing the drag by 50% but increasing the lift by 35%, the periodic flight over the cruise region is 13.27% better than when flying in steady state. Results for mechanizing the periodic flight by a linear guidance rule allow the constant vehicle weight assumption to be removed but retain the periodic cruise performance.

I. Introduction

OPTIMAL periodic cruise (fuel/range) and optimal periodic endurance (fuel/time) are developing technologies that are just beginning to be mature enough for implementation on real systems. A review of much of the relevant theoretical, numerical, and implementation literature is given in [1]. In that paper two basic mechanisms that lead to a periodic fuel efficient cruise are discussed. The first mechanism is that if the hodograph of reachable velocities in a reduced energy-height approximation is not convex at the cruise point, then the convex hull of the hodograph leads to the notion of a chattering cruise as being superior to a steady-state cruise. The second mechanism is related to an efficient kinetic-potential energy interchange. If the vehicle is moving sufficiently fast, then the periodic cruise may well be superior in fuel performance to the steady-state cruise. Therefore, hypersonic flight is a good candidate for improved cruise performance by periodic flight.

In this paper the dynamic cruise optimality of a recent hypersonic waverider design is investigated. This vehicle, described in Sec. II, is not specifically designed for periodic cruise, during which a portion of the flight the engine is turned off. During that phase the engine is either cooled by dispensing fuel or a door on the inlet is closed. These two mechanizations are realistically modeled. The optimal periodic cruise problem is formulated in Sec. III, in which the fuel used over a range period is minimized subject to system dynamics, periodic equality constraints in which the initial state is to be equal to the terminal state over a period, and control and state variable inequality constraints along the periodic trajectory. It is assumed that the vehicle weight is given and held fixed over the period. This small approximation leads to an enormous savings in numerical error and computation time. Given the functional complexity of the aerodynamic and engine data on the Mach number, angle of attack, and altitude, the control time function is parameterized and efficient parameter optimization techniques are used. The gradients of the cost and constraints with respect to all parameters are determined numerically. The resulting cost of the optimal periodic trajectory is compared with the cost of the optimal steady-state trajectory computed as described in Sec. IV, and both are given in Sec. V. The most significant result is that with a door placed over the inlet during the power-off phase where the drag penalty is 50% but the lift increases by 35%, the fuel improvement of a periodic cruise over a steady-state cruise for a reasonable vehicle weight change is 13.27%. Although the benefit of a periodic cruise was discovered in the 1970s, those results were obtained by using simple aerodynamic and engine data usually with simplifications in the equations of motion (such as small angle of attack approximation), and gravity and atmosphere models. This paper shows the improvement of a periodic cruise over a steady-state cruise in a more realistic environment.

Because these results are significant, but the periodic trajectories are more complex than the steady-state trajectories, the ease of implementation of the periodic trajectories is of some consequence. To mechanize the periodic flight, the formulation of a periodic guidance law is presented in Sec. VI which allows the constant vehicle weight assumption to be removed but retains the periodic cruise performance. One new innovation required is the determination of an index point from which the nominal values required for the guidance law are retrieved. The other new innovation is the analysis of the guidance law considering the discontinuity in the system dynamics due to turning on and off the engine. In Sec. VII the results of this mechanization are given and the optimal periodic cruise results predicted in Sec. V are nearly obtained even though the restriction on vehicle weight is now removed and the vehicle weight decrease due to fuel consumption is now exactly accounted for.

II. Hypersonic Cruise Vehicle

The point of departure configuration is the traditional scramjet design shown in Fig. 1, which is similar to the UX-30 (NASP) studied in [2]. This vehicle is designed as a cruiser around Mach 10 and low dynamic pressure (less than 1000 psf) with 12,000 lb payload and 9000 n mile range. Complete aerodynamics, including

Received 8 August 2005; revision received 2 March 2006; accepted for publication 6 March 2006.

*Principal Engineer, AIAA Member.
†CEO, AIAA Member.
‡CTO and Professor, UCLA, speyer@sysense.com, AIAA Fellow (corresponding author).
§Senior Principal Research Engineer, Advanced Development Programs, AIAA Senior Member.
‖Senior Staff Embedded Software Engineer, Advanced Development Programs, AIAA Member.

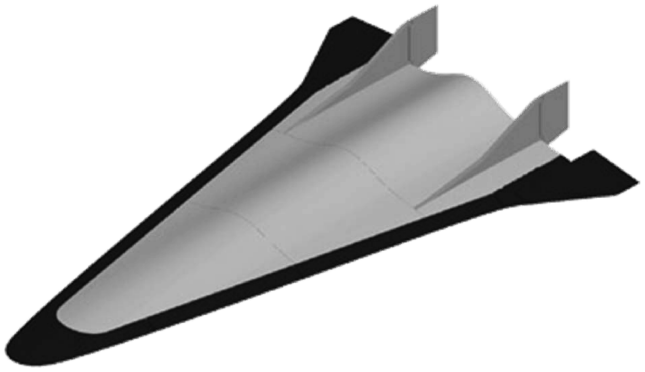

Fig. 1 Traditional scramjet configuration.

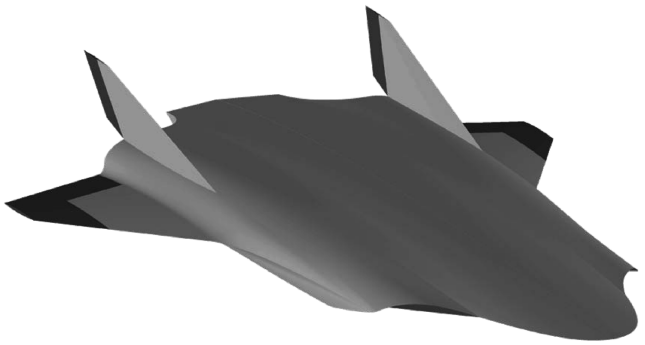

Fig. 2 Inward turning configuration.

viscous effect, integrated propulsion with airframe, weight, and thermal protection database is generated for comparison purposes with other configurations.

The preferred concept is a nontraditional configuration in which the propulsion system including the scramjet is inside the airframe with an inward turning flow path as shown in Fig. 2. The vehicle is designed to meet the same mission requirement as the other configurations. Although this vehicle is not specifically designed for periodic cruise, it has several characteristics that will potentially benefit the periodic cruise. First, the maximal lift-to-drag ratio of the vehicle is higher than the UX-30 which allows the vehicle to glide more efficiently during the power-off phase. Second, the engine is installed such that it provides normal thrust that pushes the vehicle up which acts like additional lift. Third, the thrust-to-weight ratio of the vehicle is higher than the UX-30 which allows the vehicle to ascent and leave the atmosphere faster at the bottom of the periodic trajectory. Fourth, the engine is almost equally efficient across different throttles because the curve of thrust versus fuel rate is almost a straight line. This allows the vehicle to use more thrust for the periodic cruise without reducing the engine's efficiency. Finally, the engine is more efficient [higher ISP (specific impulse)] when the dynamic pressure is higher. This favors the periodic cruise because the engine is turned on at the bottom of the periodic trajectory where the dynamic pressure is much higher than the steady-state cruise.

A complete database is generated for the vehicle and used in this paper to analyze the periodic and steady-state cruise. This database is more complicated and realistic than the ones used in previous studies such as [3]. For example, the aerodynamic and engine data are functions of the Mach number, angle of attack, and altitude. Furthermore, two different methods are used to protect the propulsion system during the power-off phase of the periodic flight: flow-through cooling and articulated door. For the first method, the engine is cooled by dispensing fuel because its components get hot from the plasma that flows through the engine. This mechanization is realistically modeled by the axial and normal thrusts and fuel rate as functions of the Mach number, angle of attack, and dynamic pressure. For the second method, a door is placed over the inlet to prevent the plasma flowing through the engine. The change in the aerodynamics because of the door is modeled by a 50% overall drag penalty and 35% additional overall lift while the axial and normal thrusts and fuel rate are zero. Note that this issue has not been realistically addressed in previous studies.

III. Optimal Periodic Cruise Problem

In this section, the optimal periodic cruise problem is formulated and solved numerically. It is assumed that the hypersonic cruise vehicle is constrained to fly in a vertical plane over a nonrotating, spherical Earth. Then, the equations of motion for the vehicle are

$$\dot{h} = v \sin\gamma \tag{1a}$$

$$\dot{v} = \frac{T_A \cos\alpha - T_N \sin\alpha - D}{m} - g \sin\gamma \tag{1b}$$

$$\dot{\gamma} = \frac{T_A \sin\alpha + T_N \cos\alpha + L}{mv} + \cos\gamma\left(\frac{v}{R_e + h} - \frac{g}{v}\right) \tag{1c}$$

$$\dot{r} = v \cos\gamma\left(\frac{R_e}{R_e + h}\right) \tag{1d}$$

The states are the altitude h, velocity v, flight path angle γ, and range r. The controls are the angle of attack α and throttle S. $L = \bar{q} S_e C_L$ is the lift and $D = \bar{q} S_e C_D$ is the drag where $\bar{q}$ is the dynamic pressure, S_e is the reference area, and C_L and C_D are the lift and drag coefficients, respectively. T_A and T_N are the axial and normal thrusts, respectively. m is the vehicle mass. g is the acceleration due to the gravity which is inversely proportional to the square of the distance between the vehicle and center of the Earth. R_e is the radius of the Earth. The 1976 U.S. standard atmosphere model is used to calculate the air density, which is used in the calculation of dynamic pressure, and temperature, which is used in the calculation of the speed of sound to determine the Mach number. For the hypersonic cruise vehicle described in Sec. II, C_L and C_D are functions of the Mach number, angle of attack, and altitude, and T_A and T_N are functions of the Mach number, angle of attack, dynamic pressure, and throttle. Furthermore, the fuel rate $\dot{m}_f$ is a function of the Mach number, angle of attack, dynamic pressure, and throttle.

The optimal periodic cruise problem is formulated as a constrained optimization problem [3]. The cost to be minimized is the ratio of the fuel consumption to the range over one period as

$$J = \frac{\int_0^T \dot{m}_f \mathrm{d}t}{\int_0^T \dot{r} \mathrm{d}t}$$

where T is the period. The control variables to be determined are $\alpha(t)$, $S(t)$, $h(0)$, $v(0)$, $\gamma(0)$, and T where $t \in [0, T]$. There are three types of constraints. The first type is the equations of motion (1). The second type is the periodic constraints where $h(T) = h(0)$, $v(T) = v(0)$, and $\gamma(T) = \gamma(0)$. The third type is the physical constraints on the vehicle. For the hypersonic cruise vehicle described in Sec. II, these constraints include $-2 \le \alpha \le 7$ deg, $\bar{q} \le 2000$ psf, and the net acceleration is less than 4 g for maintaining the structure integrity and thermal protection system, and $0.4 \le S \le 1.2$ and $\bar{q} \ge 250$ psf for operating the engine.

For the optimization problem, it is assumed that the vehicle mass is given and held fixed over the period. Note that the periodic constraints are not applicable without this assumption. Instead of formulating the optimization problem for a single period at fixed vehicle mass, one might formulate the optimization problem for the entire flight without the periodic constraints using variable vehicle mass (i.e., given initial and final vehicle masses). This will produce the trajectory for the entire flight which might be periodic or steady state. However, this is not practical because the dimension of this optimization problem will be very large because the vehicle travels more than 9000 n mile in over 2 h. Therefore, the approach used here is to approximate the large optimization problem by several small optimization problems with periodic or steady-state constraints using

constant vehicle mass assumption. This small approximation leads to an enormous savings in numerical error and computation time. Because the optimal periodic trajectories are obtained for several constant vehicle masses, a periodic guidance law is developed in Sec. VI to mechanize the periodic flight where the vehicle mass decreases as a result of fuel consumption. Note that the vehicle mass change in one period is negligible because the fuel consumed over one period for the vehicle studied in this paper is less than 1% of the vehicle mass.

Because the optimal periodic cruise problem is too complicated to be solved analytically, it is solved numerically by using a numerical parameter optimization algorithm [4]. However, the optimal periodic cruise problem is a functional optimization problem because the control variables include the time histories of the angle of attack and throttle. To convert it into a parameter optimization problem, the angle of attack and throttle are parameterized so that the number of control variables is finite and fixed [5]. The physical constraints on the vehicle are also parameterized so that the number of constraints is finite and fixed. For the numerical algorithm, the gradients of the cost and constraints with respect to the control variables are determined numerically. Furthermore, the cost and states are obtained by integrating the equations of motion (1) with linear interpolation between the parameterized angle of attack and throttle. Finally, the optimization problem is divided into two phases. The first phase is the coasting phase where the engine is turned off. During this phase, the control variables are α, $h(0)$, $v(0)$, $\gamma(0)$, and T_1, the duration of the first phase. The constraints are $-2 \le \alpha \le 7$ deg, $\bar{q} \le 2000$ psf and the net acceleration is less than 4 g. The second phase is the boost phase where the engine is turned on. During this phase, the control variables are α, S, and T_2, the duration of the second phase. The constraints are $-2 \le \alpha \le 7$ deg, $0.4 \le S \le 1.2$, $250 \le \bar{q} \le 2000$ psf, the net acceleration is less than 4 g, $h(T_1 + T_2) = h(0)$, $v(T_1 + T_2) = v(0)$, and $\gamma(T_1 + T_2) = \gamma(0)$. The numerical results are shown in Sec. V.

To confirm the solution obtained, OTIS [6] is also used to solve the optimal periodic cruise problem. The solutions obtained by these two numerical algorithms are reasonably close. Note that these solutions are only local minima and may not be the global minimum. There are two major differences between the two numerical algorithms. First, OTIS is based on the sequential quadratic programming method [5,7], while our numerical algorithm [4] is based on the accelerated gradient projection method [8–10]. Second, OTIS uses the collocation method to approximate the equations of motion as part of the optimization problem [5,6] while our numerical algorithm integrates the equations of motion.

IV. Optimal Steady-State Cruise Problem

In this section, the optimal steady-state cruise problem is formulated as a constrained optimization problem where the instantaneous fuel rate per distance is minimized subject to the dynamics being in equilibrium and the physical constraints on the vehicle. From (1), the equations of motion in equilibrium are

$$0 = T_A \cos\alpha - T_N \sin\alpha - D \tag{2a}$$

$$0 = T_A \sin\alpha + T_N \cos\alpha + L - mg + \frac{mv^2}{R_e + h} \tag{2b}$$

$$\dot{r} = \frac{vR_e}{R_e + h} \tag{2c}$$

with the flight path angle being zero. By using (2c), the instantaneous fuel rate per distance is

$$\frac{\mathrm{d}m_f}{\mathrm{d}r} = \frac{\dot{m}_f}{\dot{r}} = \frac{\dot{m}_f(R_e + h)}{vR_e}$$

Therefore, the optimal steady-state cruise problem is

$$\min_{\alpha,S,h,v} \frac{\dot{m}_f(R_e + h)}{vR_e}$$

subject to (2a) and (2b), and the physical constrains on the vehicle that include $-2 \le \alpha \le 7$ deg, $0.4 \le S \le 1.2$, and $250 \le \bar{q} \le 2000$ psf. Because the optimal steady-state cruise problem minimizes the instantaneous fuel rate at certain vehicle mass, it has to be solved for several vehicle masses. Note that the constant vehicle mass assumption used in the optimal periodic cruise problem can be interpreted similarly with this point of view. Furthermore, a guidance law is required to mechanize the steady-state flight similar to the periodic flight.

Because the optimal steady-state cruise problem is too complicated to be solved analytically, it is solved numerically. Note that the optimal steady-state cruise problem is a parameter optimization problem with four control variables and two equality constraints. Because the degree of freedom of the optimization problem is only two, a global search method is used to solve the optimization problem. First, by specifying the altitude and velocity, the degree of freedom of the optimization problem becomes zero and the problem becomes solving (2a) and (2b) for the angle of attack and throttle. The optimization toolbox of MATLAB is used to solve this two-dimensional equation. Alternatively, other numerical algorithms for solving equations such as the Newton–Raphson method can be used [11]. Then, the cost can be obtained for the specified altitude and velocity. By performing this procedure for a range of altitude and velocity over the possible flight envelope, the cost can be constructed as a two-dimensional curve versus altitude and velocity. Essentially, this converts the constrained optimization problem into an unconstrained optimization problem as

$$\min_{h,v} \frac{\dot{m}_f(R_e + h)}{vR_e}$$

where α and S are functions of h and v. Finally, the minimum of the curve within the region that satisfies the physical constraints on the vehicle can be obtained. Although the global search method is numerically inefficient, the solution obtained for the optimal steady-state cruise problem is the global minimum. The numerical results are shown in Sec. V.

V. Numerical Results

In this section, the solution of the optimal periodic cruise problem is compared to the solution of the optimal steady-state cruise problem. Because both optimization problems assume constant vehicle mass, the solutions are obtained for four different vehicle weights at 200, 250, 300, and 350 klb. For the optimal steady-state cruise problem, the minimal cost for each vehicle weight is shown in the second column of Table 1. An example for the cost as a two-dimensional curve versus altitude and velocity when the vehicle

Table 1 Minimal costs for optimal steady state and periodic cruise

Vehicle weight, klb	Steady state cost, lb/n mile	Periodic cost: cooling (lb/n mile)	Periodic cost: 25% cooling, lb/n mile	Periodic cost: door, lb/n mile
200	12.53	11.77 (6.07%)	10.47 (16.44%)	9.67 (22.83%)
250	13.54	NA	12.82 (5.32%)	11.92 (11.96%)
300	15.42	NA	15.34 (0.52%)	14.18 (8.04%)
350	17.03	NA	NA	16.31 (4.23%)

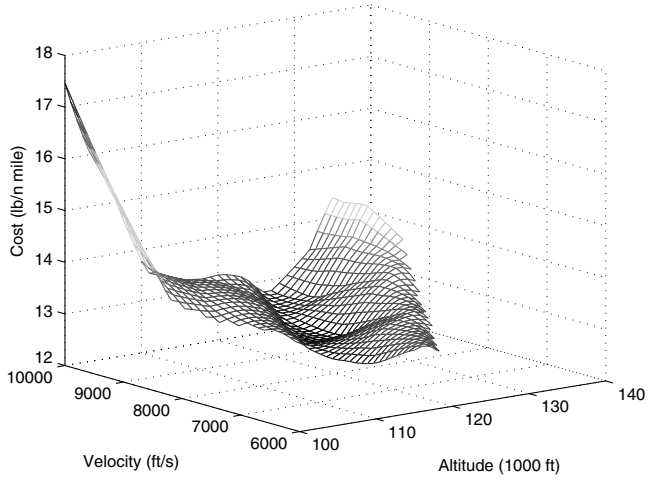

Fig. 3 Steady state cost versus altitude and velocity.

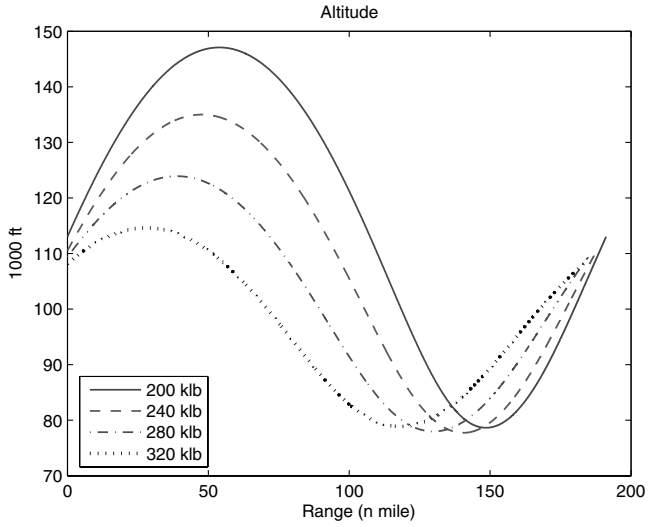

Fig. 4 Optimal periodic trajectories: altitude.

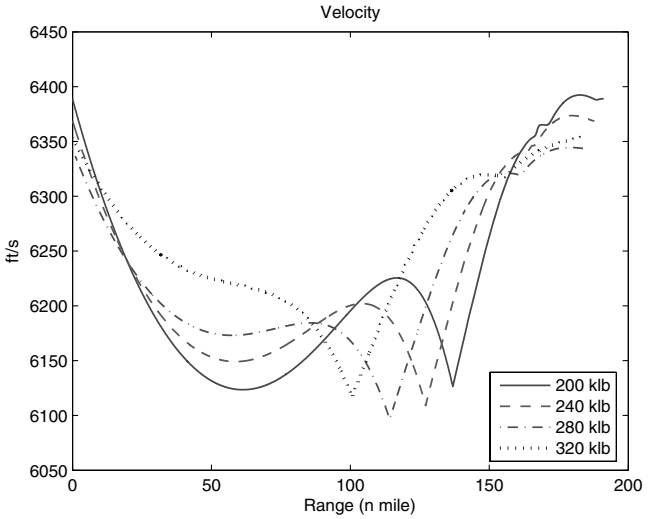

Fig. 5 Optimal periodic trajectories: velocity.

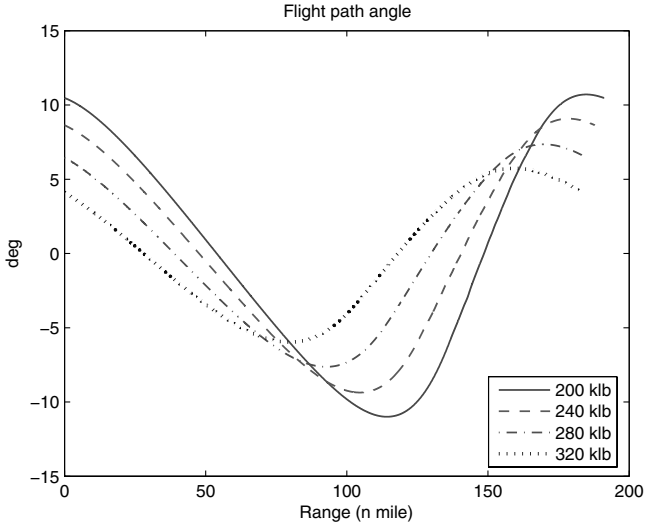

Fig. 6 Optimal periodic trajectories: flight path angle.

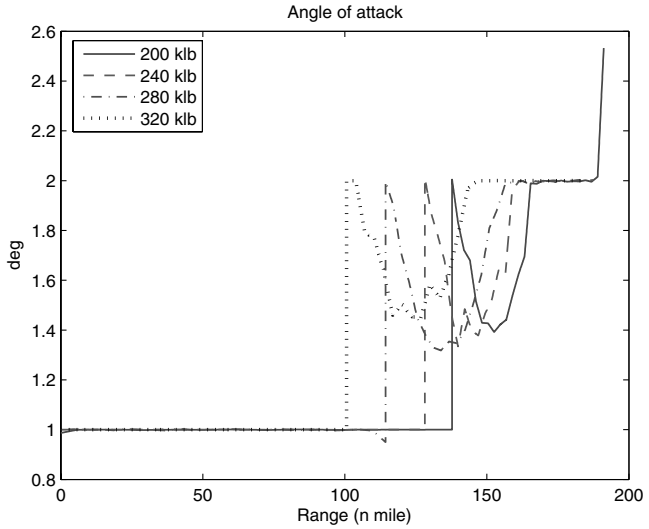

Fig. 7 Optimal periodic trajectories: angle of attack.

weight is 200 klb is shown in Fig. 3. The optimal steady-state trajectory is shown in Sec. VII.

For the optimal periodic cruise problem, three sets of solutions are obtained. The first set is for the case where the engine is cooled by dispensing fuel during the coasting phase. The minimal cost and the improvement over steady-state cost (in parentheses) for each vehicle weight are shown in the third column of Table 1. "NA" indicates that no periodic solution can be found that has a smaller cost than the steady-state cost. For this case, the periodic cruise does not perform well because the fuel required to cool off the engine seems too conservative in that it is 41–87% of the fuel required to maintain the minimal throttle. Therefore, the second set of solutions are obtained where the fuel required to cool off the engine is reduced to 25% of its original value. The minimal cost and the improvement over steady-state cost (in parentheses) for each vehicle weight are shown in the fourth column of Table 1.

The third set of solutions are for the case where a door is placed over the inlet during the coasting phase. The minimal cost and the improvement over the steady-state cost (in parentheses) for each vehicle weight are shown in the fifth column of Table 1. For this case, the periodic cruise outperforms the steady-state cruise noticeably. If the vehicle weight is 150 klb, the improvement is at 34.65%. Note that these results are conservative in that the steady-state solutions are global minima whereas the periodic solutions may only be local minima. The optimal periodic trajectories for this case are shown in Figs. 4–8 with periods ranging from 179.3 to 189.2 s. Finally, the stagnation heat load and heat rate for the optimal steady-state and periodic cruises are compared when the vehicle weight is 200 klb. Figure 9 shows that the heat load of the optimal periodic cruise is 29.73% lower than that of the optimal steady-state cruise for traveling the same amount of range whereas the maximal heat rate of

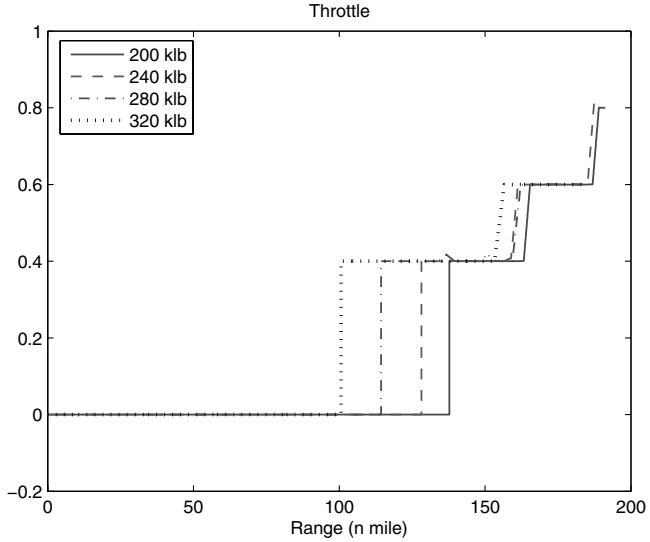

Fig. 8 Optimal periodic trajectories: throttle.

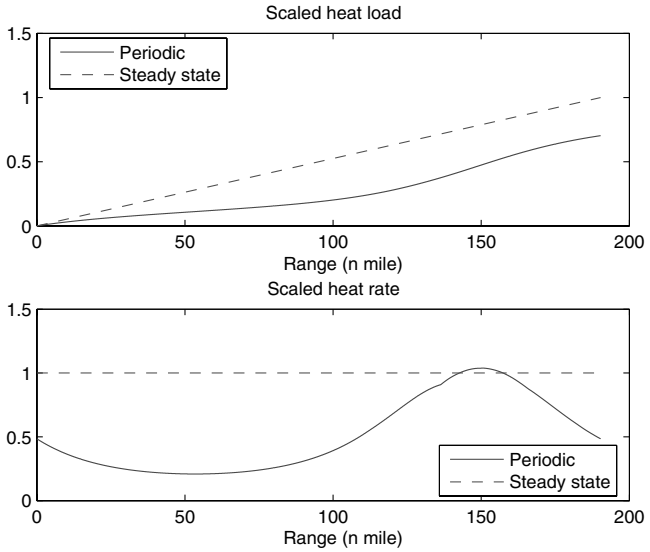

Fig. 9 Scaled heat load and heat rate for optimal steady state and periodic cruise.

the optimal periodic cruise is only 3.81% higher than that of the optimal steady-state cruise.

Now the total range that the vehicle can travel from 330 klb, the vehicle weight when the vehicle finishes climbing and is ready to cruise, to 210 klb, the vehicle weight when the vehicle prepares to land, is obtained. Figure 10 shows the inverse of the steady-state and periodic costs that are summarized in Table 1 versus the vehicle weight. Because the total range is the area underneath the curve between the two vehicle weights, the total range is obtained by integrating the inverse of the cost with respect to the vehicle weight from 210 to 330 klb. During the integration, the cost is linearly interpolated with the vehicle weight. The total range for the optimal steady-state cruise is 8390.9 n mile. The total range for the optimal periodic cruise where the fuel required to cool off the engine during the coasting phase is reduced to 25% is 8828.5 n mile and the improvement over the optimal steady-state cruise is 5.21%. For this case, the vehicle flies in steady state for a portion of the flight between the vehicle weight of 300 and 350 klb because the steady-state cruise is more fuel efficient than the periodic cruise at 350 klb. Finally, the total range for the optimal periodic cruise where a door is placed over the inlet during the coasting phase is 9504.6 n mile and the improvement over the optimal steady-state cruise is 13.27%. This shows that there is a significant improvement of the periodic cruise over the steady-state cruise for the hypersonic cruise vehicle described in Sec. II.

VI. Periodic Guidance Law

In this section, a periodic guidance law is derived to mechanize the periodic flight that allows the constant vehicle mass assumption used for generating the optimal periodic trajectories to be removed but retains the periodic cruise performance. In Sec. VI.A, the periodic guidance law is formulated. In Sec. VI.B, the periodic guidance law is analyzed considering the discontinuity in the system dynamics due to turning on and off the engine.

A. Guidance Law Formulation

In this section, a periodic regulator is first derived for each optimal periodic trajectory. Then, a periodic guidance law is formulated based on a group of periodic regulators to handle the decreasing vehicle mass due to fuel consumption. For notational convenience, let states x and controls u be

$$x \triangleq \begin{bmatrix} h \\ v \\ \gamma \end{bmatrix}, \qquad u \triangleq \begin{bmatrix} \alpha \\ S \end{bmatrix}$$

Then, the equations of motion (1) can be expressed as

$$\dot{x} = f(x, u) \tag{3}$$

Note that the range is not included because it does not need to be tracked and is decoupled from (3). Denote the states and controls associated with the optimal periodic trajectory (also referred to as the nominal trajectory) as x_N and u_N, respectively. To keep the vehicle on the nominal trajectory (i.e., to regulate $x - x_N$), a periodic regulator is designed for each nominal trajectory.

First, the equations of motion (3) are linearized around the nominal trajectory to obtain the linearized dynamics as

$$\delta\dot{x}(t) = A(t)\delta x(t) + B(t)\delta u(t) \tag{4}$$

where $\delta x = x - x_N$, $\delta u = u - u_N$, and

$$A = \left.\frac{\partial f}{\partial x}\right|_{x=x_N, u=u_N}, \qquad B = \left.\frac{\partial f}{\partial u}\right|_{x=x_N, u=u_N}$$

Note that the linearized dynamics is periodic, that is, $A(t+T) = A(t)$ and $B(t+T) = B(t)$ where T is the period of the nominal trajectory. Then, the periodic linear quadratic regulator problem can be formulated as

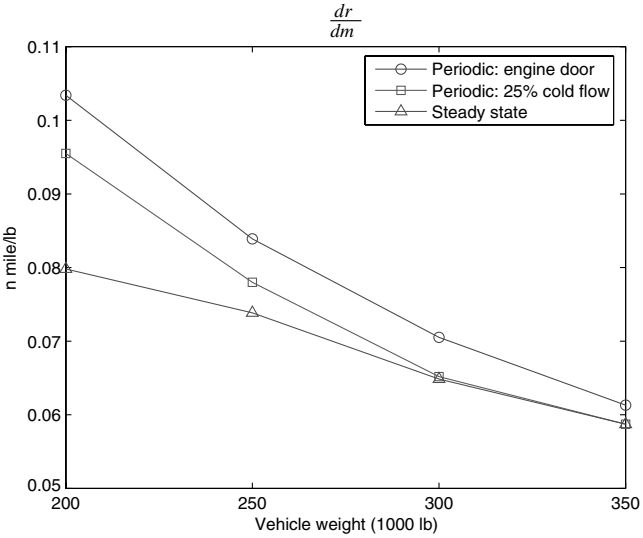

Fig. 10 Inverse of costs for optimal steady state and periodic cruise.

$$\lim_{n\to\infty}\min_{\delta u(t)}\frac{1}{nT}\int_0^{nT}\frac{1}{2}[\delta x(t)^T Q\delta x(t)+\delta u(t)^T R(t)\delta u(t)]\mathrm{d}t$$

subject to (4) where $Q>0$ and $R>0$ are design weightings [12]. By using calculus of variations [13], the optimal solution is

$$\delta u(t)=K(t)\delta x(t)$$

where the regulator gain is

$$K(t)=-R(t)^{-1}B(t)^T\Pi(t)$$

In [14], it is shown that there exists a periodic equilibrium (unique and positive definite solution) for the associated Riccati equation as $n\to\infty$ if (A,B) is controllable and the monodromy matrix (the state transition matrix evaluated over one period) has no eigenvalues on the unit circle. Therefore, the Riccati matrix Π satisfies the periodic Riccati equation.

$$-\dot{\Pi}(t)=\Pi(t)A(t)+A(t)^T\Pi(t)-\Pi(t)B(t)R(t)^{-1}B(t)^T\Pi(t)+Q$$
$$\Pi(0)=\Pi(T)$$

Because the periodic regulator is defined on the nominal trajectory and the vehicle may not be on the nominal trajectory, an index point is defined from which the nominal values (i.e., x_N, u_N, and K) required for the periodic regulator are retrieved. The index point can be defined as the point on the nominal trajectory whose states (i.e., x_N) are closest to the current states (i.e., x) in terms of certain criterion. Then, by indexing the nominal trajectory with time, the index time t_I of the index point can be obtained by solving

$$\min_{t_I\in[0,T]}[x(t)-x_N(t_I)]^T\bar{Q}[x(t)-x_N(t_I)]$$

where $\bar{Q}>0$ is a design weighting for normalizing the states which could be chosen equal to Q. Alternatively, the index time can be obtained by solving

$$\dot{x}_N(t_I)^T\bar{Q}[x(t)-x_N(t_I)]=0$$

After using the current states x to determine the index time t_I, the nominal states x_N, nominal controls u_N, and regulator gain K can be obtained to generate the controls u that will keep the vehicle on the nominal trajectory (i.e., $\delta x\to 0$).

After designing the periodic regulators for a group of optimal periodic trajectories associated with a range of vehicle mass, the periodic guidance law is formulated based on these periodic regulators in order to handle the decreasing vehicle mass. First, given the current vehicle mass, the index time on each of the two nominal trajectories associated with the next heavier and lighter vehicle masses is determined. Next, the nominal states, nominal controls, and regulator gain on each nominal trajectory are determined. Then, the nominal states, nominal controls, and regulator gain for the current vehicle mass are determined by linear interpolating between the next heavier and lighter vehicle masses using the current vehicle mass. Finally, the controls that will keep the vehicle on the interpolated nominal trajectory are determined. The periodic guidance law for mechanizing the optimal periodic cruise is summarized in Fig. 11.

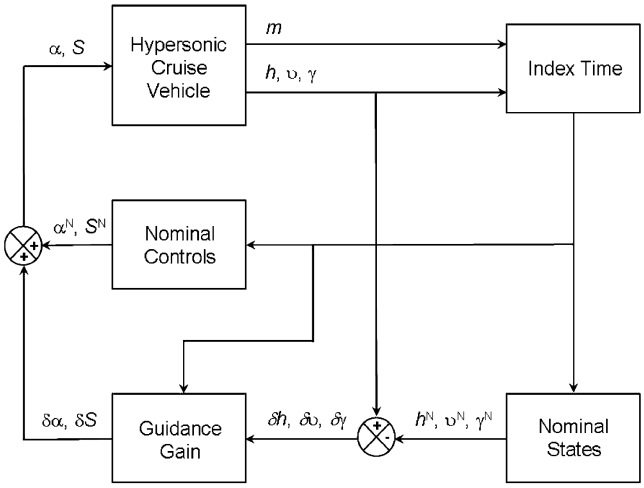

Fig. 11 Periodic guidance law.

B. Guidance Law Analysis

Because the nominal trajectories have a discontinuity in the throttle as the trajectory passes through a given value of dynamic pressure or the optimality condition on the throttle goes through zero, the associated guidance law has to reflect this discontinuity. The engine is turned off for dynamic pressures below the threshold value (250 psf) or the optimality condition is negative. Our analysis indicates that the guidance gains for this discontinuity associated with the linearized equations of motion about the nominal path *are* continuous. However, care must be taken in defining the perturbation in the states away from the nominal path in the vicinity of the discontinuity. In Sec. I, the nominal path and the nature of the discontinuity are described. In Sec. II, the perturbation dynamics are stated and the effect of the discontinuity of the nominal path on the guidance gain calculations is discussed.

1. *Description of the Nominal Path*

Assume the switching function associated with dynamic pressure or the optimality condition on the throttle is in the form of $\Omega(x,t)$. Consider the dynamic system for the vehicle as

$$\dot{x}=f_1(x,u),\qquad \Omega(x,t)\geq 0\qquad \dot{x}=f_2(x,u),\qquad \Omega(x,t)<0$$

where $f_1(x,u)$ and $f_2(x,u)$ indicate the dynamic system when $\Omega(x,t)$ is either positive or negative, respectively. Consider that δx is "close" to the nominal path such that the perturbed states are defined as

$$\delta x(t)=x(t)-x_N(t_I)$$

where t_I, the index time, is determined by finding the orthogonal value of $\delta x(t)$ to the tangent of the nominal path where the tangent is represented as f_1 or f_2 depending on the sign of the switch function $\Omega(x,t)$. However, when $\Omega(x,t)=0$, the switch time t_s can be used rather than t_I. Note that if $t\leq t_s$ $(t>t_s)$, then the controls for the nominal dynamics before (after) the switch are used.

2. *Perturbation Guidance with Discontinuous Control in the Nominal Path*

The perturbed system dynamics are represented by the linear differential equations

$$\delta\dot{x}(t)=A_1(t)\delta x(t)+B_1(t)\delta u(t)\triangleq\tilde{f}_1(\delta x,\delta u)$$

when $\Omega(x,t_s)\geq 0$ or approximately $\Omega[x^N(t_I),t_I]+\Omega_x[x^N(t_I),t_I]\,\delta x(t)\geq 0$ and

$$\delta\dot{x}(t)=A_2(t)\delta x(t)+B_2(t)\delta u(t)\triangleq\tilde{f}_2(\delta x,\delta u)$$

when $\Omega[x^N(t_I),t_I]+\Omega_x[x^N(t_I),t_I]\delta x(t)<0$ where $\delta u(t)=u(t)-u_N(t_I)$, $\Omega_x=\frac{\partial\Omega}{\partial x}$, and t_I is the index time away from the switch curve and becomes the nominal switch time t_s^N when either the switch curve or the optimality condition is reached. Let Ω pass from positive to negative and the superscripts "$-$" and "$+$" denote the positive and negative sides of Ω, respectively. Then, the perturbation about t_s^N is defined as

$$\delta x(t)\triangleq \mathrm{d}x(t)=\delta x^-(t_s^N)+f_1(t_s^N)\mathrm{d}t \tag{5}$$

where $\mathrm{d}t=t-t_s^N$. At the switch time $\Omega(x,t_s)=0$ and to first order using (5),

$$\Omega(x, t_s) = \Omega_t\left(t_s^N\right)\mathrm{d}t_s + \Omega_x\left(t_s^N\right)\mathrm{d}x(t_s)$$
$$\cong \Omega_t\left(t_s^N\right)\mathrm{d}t_s + \Omega_x\left(t_s^N\right)\left[\delta x^-\left(t_s^N\right) + f_1\left(t_s^N\right)\mathrm{d}t_s\right] = 0$$

where $\mathrm{d}t_s = t_s - t_s^N$, $\Omega_t = \frac{\partial\Omega}{\partial t}$, and f_1 denotes the side of the nominal path just before the switch function changes from positive to negative. Therefore, the change in time of the switch is

$$\mathrm{d}\,t_s = -\left[\Omega_t\left(t_s^N\right) + \Omega_x\left(t_s^N\right)f_1\left(t_s^N\right)\right]^{-1}\Omega_x\left(t_s^N\right)\delta x^-\left(t_s^N\right)$$

Now the behavior of the guidance gains as they pass across the switch point are to be determined. The guidance gains at the switch point are

$$K\left(t_s^N\right) = -R\left(t_s^N\right)^{-1}B_i\left(t_s^N\right)^T\Pi\left(t_s^N\right)$$

where $R(t_s^N)$ is assumed continuous, $i = 1$ or 2 depending if Ω is passing from positive to negative or vise versa and $B_i(t_s^N)$ may be discontinuous across the switch point. Since no optimality of the switch time is assumed for the linear quadratic regulator used here, the Riccati matrix Π is continuous across the switch time [15].

3. Algorithmic Considerations of the Guidance Law in the Vicinity of the Nominal Discontinuity

If the perturbed trajectory reaches the optimality condition on the throttle before the $\Omega(x, t) = 0$ condition, we switch to the nominal path on the other side of the discontinuity. If the perturbed trajectory reaches the $\Omega(x, t) = 0$ condition before the optimality condition on the throttle, the following two cases are considered. Suppose that as the nominal path is traversed, the index time, obtained by our algorithm, does not reach the nominal discontinuity before the perturbed trajectory reaches the $\Omega(x, t) = 0$ condition. Once the equality condition is reached, we switch to the nominal path on the other side of the discontinuity. Suppose that as the nominal path is traversed, the index time, obtained by our algorithm, does reach the nominal discontinuity before the perturbed trajectory reaches the $\Omega(x, t) = 0$ condition. It is suggested that the index time remains at the discontinuity using the nominal states at the discontinuity until the constraint equality is reached. Then, we switch to the nominal path on the other side of the discontinuity. If again the index time, obtained by our algorithm, resides at the discontinuity, the nominal states at the discontinuity are used.

VII. Mechanization of Optimal Periodic Cruise

In this section, the periodic guidance law formulated in Sec. VI is implemented to mechanize the periodic flight. First, eight optimal periodic trajectories are generated at vehicle weights of 200, 220, 240, 260, 280, 300, 320, and 340 klb for the case where a door is placed over the inlet during the coasting phase. Then, eight periodic regulators are designed for these eight vehicle weights. Finally, the periodic guidance law consisting of these eight periodic regulators is implemented to mechanize the periodic flight from the vehicle weight of 330–210 klb. The total range of the periodic flight is 9578.4 n mile compared to the theoretic value of 9504.6 n mile obtained in Sec. V. Note that the total range of the periodic flight mechanized by the periodic guidance law depends on where the periodic flight starts along the periodic trajectory. For example, the total range of 9578.4 n mile is obtained when the periodic flight starts near the beginning of the coasting phase. If the periodic flight starts at the beginning of the boost phase, the total range will be 97.4 n mile shorter.

The complete periodic flight is shown in Figs. 12–17 along with the steady-state flight. Note that the steady-state trajectory shown is the solution of the optimal steady-state cruise problem rather than the result of using a steady-state guidance law. This explains the zero flight path angle of the steady-state trajectory as shown in Fig. 14 even though the altitude of the steady-state trajectory gradually increases as shown in Fig. 12. Part of the periodic flight from a vehicle weight of 222–210 klb is shown in Figs. 18–20. By comparing the periodic trajectory generated by using the periodic guidance law in Figs. 12–14 to the optimal periodic trajectories generated at several constant vehicle masses in Figs. 4–6, the periodic guidance law tracks the optimal periodic trajectories very

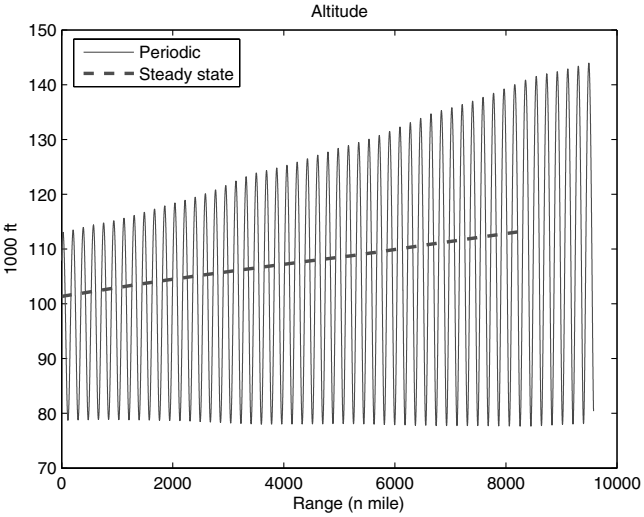

Fig. 12 Complete optimal periodic trajectory: altitude.

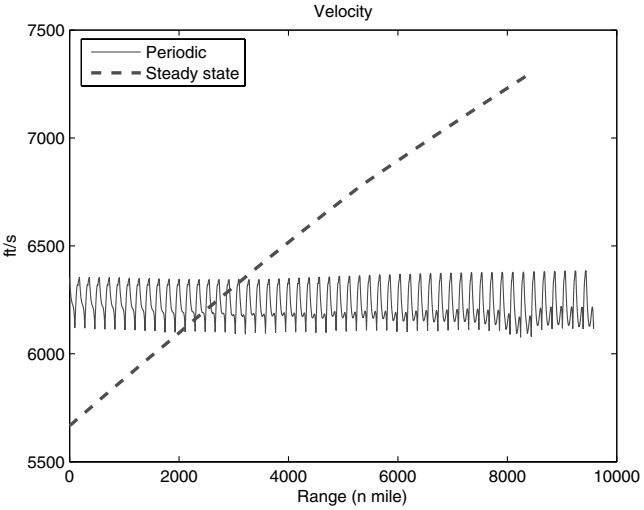

Fig. 13 Complete optimal periodic trajectory: velocity.

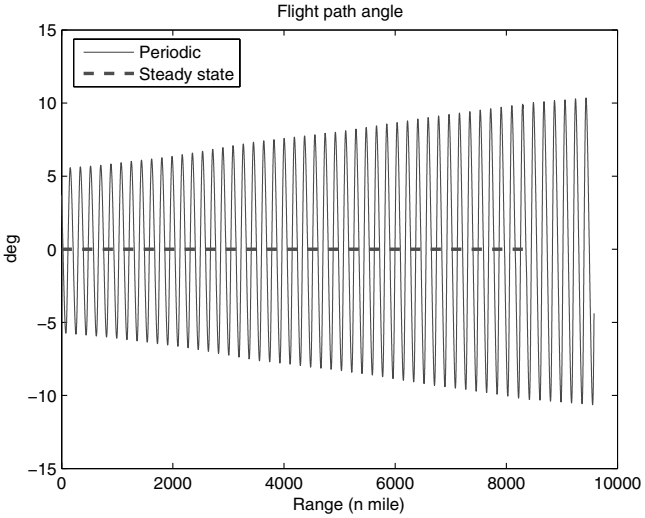

Fig. 14 Complete optimal periodic trajectory: flight path angle

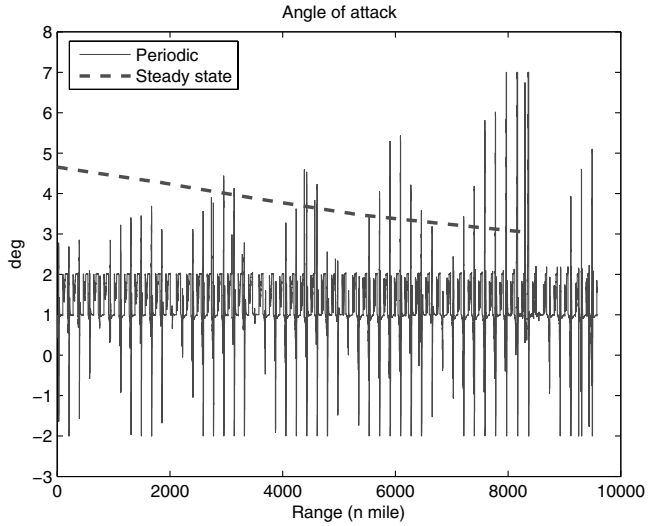

Fig. 15 Complete optimal periodic trajectory: angle of attack.

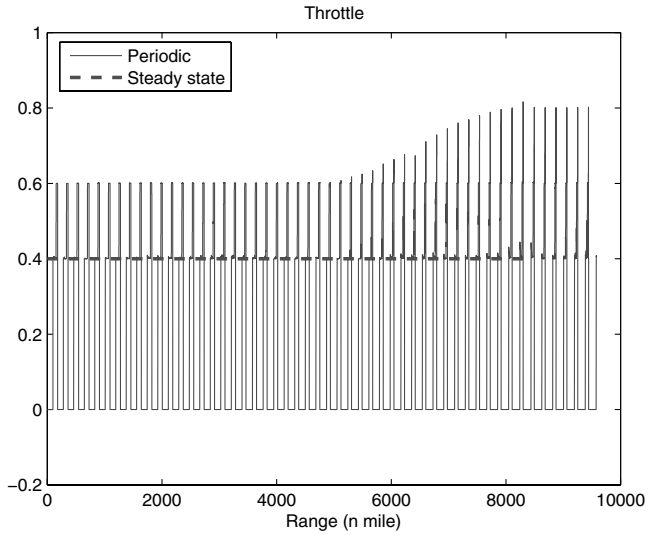

Fig. 16 Complete optimal periodic trajectory: throttle.

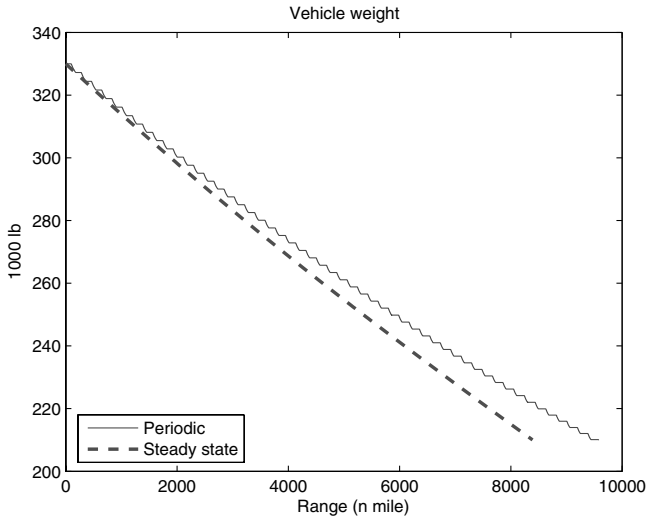

Fig. 17 Complete optimal periodic trajectory: vehicle weight.

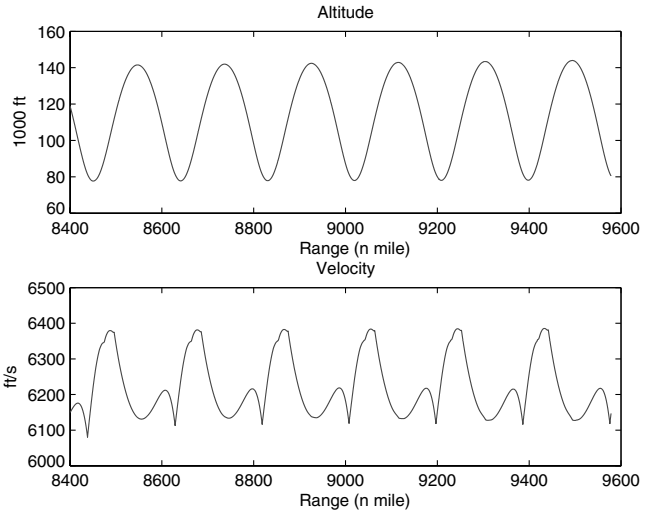

Fig. 18 Altitude and velocity from vehicle weight 222–210 klb.

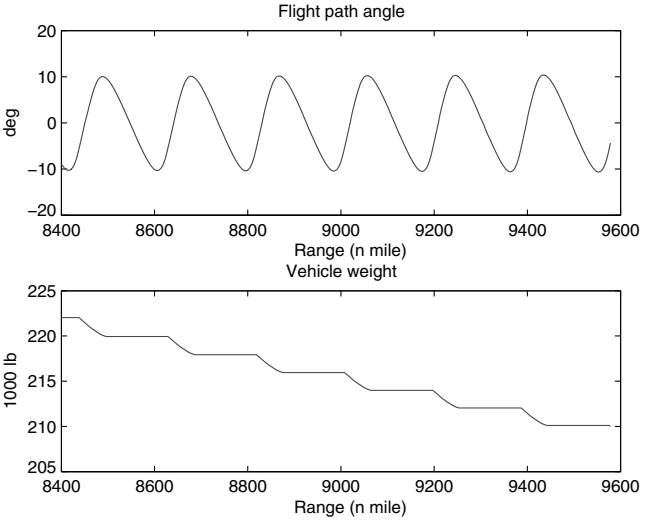

Fig. 19 Flight path angle and vehicle weight from vehicle weight 222–210 klb

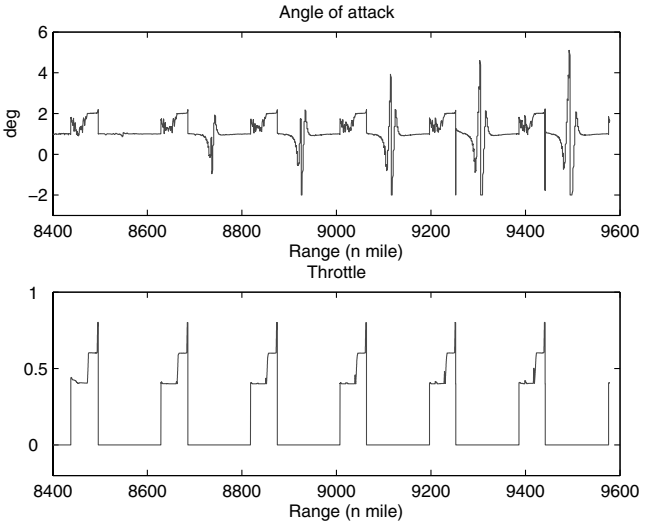

Fig. 20 Angle of attack and throttle from vehicle weight 222–210 klb

well even though the vehicle weight decreases because of fuel consumption. However, by comparing Fig. 15 to Fig. 7 there are seven regions where the periodic guidance law has to modulate the angle of attack considerably compared to the nominal angle of attack. These regions occur around the vehicle weight of 210, 230, 250, 270, 290, 310, and 330 klb which are at the middle of the design points for generating the optimal periodic trajectories. Therefore, by using more design points, the angle of attack generated by the periodic

guidance law will be closer to the nominal angle of attack. Note that the throttle generated by the periodic guidance law is very close to the nominal throttle as shown in Figs. 8 and 16.

From Figs. 12 and 13, the steady-state flight has higher altitude and faster velocity as the vehicle weight decreases. From Figs. 4 and 12, the periodic flight has a similar phenomenon of higher altitude as the vehicle weight decreases. Furthermore, from Figs. 6 and 14, the periodic flight has larger oscillation as the vehicle weight decreases because the thrust-to-weight ratio improves. However, from Figs. 5 and 13, the velocity of the periodic flight stays in a narrow range and is not as sensitive to the vehicle weight. Furthermore, the velocity is near the lower Mach number of a hypersonic flight. This is because the ISP of the engine decreases considerably as the velocity increases even taking into account that faster velocity will produce more range. Finally, from Fig. 8, rather than using a bang-bang throttle between 0 representing engine off and 1.2 representing full throttle as one would expect, the throttle is at 0.4 or 0.6 for most of the boost phase. This is because the drag penalty associated with the door placed over the inlet during the coasting phase is significant on the cruise performance. If this penalty is removed, then the periodic flight will use a bang-bang throttle between 0 and 0.6. Note that the full throttle is not used because the highest ISP is at throttle of 0.6. Therefore, by using minimal throttle of 0.4 for part of the boost phase, the duration of the coasting phase is reduced and so is the effect of the drag penalty on the cruise performance.

Although there are many factors that affect whether a periodic cruise will have improvement over a steady-state cruise such as lift-to-drag ratio, thrust-to-weight ratio, and others as described in Sec. II, the underlining physics is that the periodic cruise can fly at best aerodynamic efficiency (maximal lift-to-drag ratio) during the coasting phase and at best engine efficiency (highest ISP) during the boost phase while the steady-state cruise generally cannot fly simultaneously at best aerodynamic and engine efficiency. This allows the improvement of a periodic cruise over a steady-state cruise and this occurs to the vehicle studied in this paper. From Fig. 7, the periodic cruise flies at maximal lift-to-drag ratio during the coasting phase. From Fig. 8, the periodic cruise flies at best engine efficiency during the boost phase (ISP is slightly higher for throttle from 0.4 to 0.8 with a slight peak at 0.6 than throttle from 0.8 to 1.2). From Figs. 15 and 16, the steady-state cruise flies at the best engine efficiency but far from the best aerodynamic efficiency. This is why this vehicle performs better with periodic cruise rather than steady-state cruise.

VIII. Conclusion

Although the benefit of periodic cruise was discovered in the 1970s, the results were obtained by using simple aerodynamic and engine data usually with simplifications in the equations of motion and gravity and atmosphere models. This paper shows that in a much more realistic environment there still is significant improvement of a periodic cruise over a steady-state cruise in a detail designed hypersonic waverider vehicle that has more realistic aerodynamic and engine data and mechanizations for the power-off phase. In addition to the fuel efficiency improvement, the other benefit of the periodic cruise is the significant decrease in stagnation heat load with a slight increase in stagnation heat rate. Finally, it is shown that the periodic flight can be mechanized by the periodic guidance law while the predicted periodic cruise performance is retained.

Acknowledgment

This work was partially supported by DARPA Contract No. DAA H01-03-C-R234.

References

[1] Speyer, J. L., "Periodic Optimal Flight," *Journal of Guidance, Control, and Dynamics*, Vol. 19, No. 4, July–Aug. 1996, pp. 923–932.

[2] Youssef, H., and Chowdhry, R., "Hypersonic Global Reach Trajectory Optimization," AIAA Paper 2004-5167, 2004.

[3] Dewell, L. D., and Speyer, J. L., "Fuel-Optimal Periodic Control and Regulation in Constrained Hypersonic Flight," *Journal of Guidance, Control, and Dynamics*, Vol. 20, No. 5, Sep.–Oct. 1997, pp. 923–932.

[4] Speyer, J. L., Kelley, H. J., Levine, N., and Denham, W. F., "Accelerated Gradient Projection Technique with Application to Rocket Trajectory Optimization," *Automatica*, Vol. 7, No. 1, Jan. 1971, pp. 37–43.

[5] Betts, J. T., *Practical Methods for Optimal Control Using Nonlinear Programming*, Society for Industrial and Applied Mathematics, Philadelphia, 2001, pp. 1–52, 89–92.

[6] Hargraves, C. R., and Paris, S. W., "Direct Trajectory Optimization Using Nonlinear Programming and Collocation," *Journal of Guidance, Control, and Dynamics*, Vol. 10, No. 4, July–Aug. 1987, pp. 338–342.

[7] Gill, P. E., Murray, W., and Saunders, M. A., "SNOPT: An SQP Algorithm for Large-Scale Constrained Optimization," *SIAM Journal on Optimization*, Vol. 12, No. 4, 2002, pp. 979–1006.

[8] Rosen, J. B., "The Gradient Projection Method for Nonlinear Programming. Part I. Linear Constraints," *Journal of the Society for Industrial and Applied Mathematics*, Vol. 8, No. 1, March 1960, pp. 181–217.

[9] Rosen, J. B., "The Gradient Projection Method for Nonlinear Programming. Part II. Nonlinear Constraints," *Journal of the Society for Industrial and Applied Mathematics*, Vol. 9, No. 4, Dec. 1961, pp. 514–532.

[10] Fletcher, R., and Powell, M. J. D., "A Rapidly Convergent Descent Method for Minimization," *Computer Journal*, Vol. 6, No. 2, July 1963, pp. 163–168.

[11] Press, W. H., Teukolsky, S. A., Vetterling, W. T., and Flannery, B. P., *Numerical Recipes in C*, Cambridge Univer. Press, Cambridge, U.K., 1992, pp. 379–383.

[12] Bittanti, S., Laub, A. J., and Willems, J. C. (eds.), *The Riccati Equation*, Springer–Verlag, Berlin, 1991, pp. 127–162.

[13] Bryson, A. E., and Ho, Y.-C., *Applied Optimal Control: Optimization, Estimation, and Control*, Hemisphere, Washington, D.C., 1975, pp. 148–153.

[14] Shayman, M. A., "On the Phase Portrait of the Matrix Riccati Equation Arising from the Periodic Control Problem," *SIAM Journal on Control and Optimization*, Vol. 23, No. 5, Sept. 1985, pp. 717–751.

[15] Dyer, P., and McReynolds, S. R., *The Computation and Theory of Optimal Control*, Academic Press, New York, 1970, pp. 184–189.